



Far field detection of terahertz near field enhancement of sub-wavelength slits using Kirchhoff integral formalism

J.S. Kyoung^{*}, M.A. Seo, H.R. Park, K.J. Ahn, D.S. Kim

Center for Subwavelength Optics and Department of Physics and Astronomy, Seoul National University, Seoul 151-747, Republic of Korea

ARTICLE INFO

Article history:

Received 26 February 2010

Received in revised form 4 June 2010

Accepted 3 August 2010

Keywords:

Terahertz

Field enhancement

Kirchhoff integral

ABSTRACT

We demonstrate that the near field enhancement of sub-wavelength slits can be experimentally determined in the far field by using a reference aperture. Our simple model derived from the Kirchhoff integral formalism shows that enhancement of the near field at a slit exit with respect to the incident wave can be read in the transmitted amplitude through the slit attached on a reference aperture, normalized by the transmitted amplitude through the reference aperture. Furthermore, the near field enhancement obtained in such a way is essentially independent of the reference aperture size. By performing terahertz time domain spectroscopy we experimentally confirm the inverse frequency dependence of the near field enhancement of extremely narrow slits and measure the maximum field enhancement reaching 200 at 0.1 THz for a 500-nm-width slit.

© 2010 Elsevier B.V. All rights reserved.

1. Introduction

Periodic arrays of holes perforated in metal films have attracted considerable interests in the aspect of enhanced transmission [1–3]. Even in terahertz (THz) frequency regime where most novel metals are considered as electrically ideal conductor, perfect transmission through periodic sub-wavelength hole arrays in micron-scale has been reported [4–7]. In addition to periodicities of hole arrays, which are one of the important factors for the perfect transmission, many researches demonstrate that individual shapes of rectangles can even induce enhanced transmission [5,8–13]. Recently extra ordinary far field transmissions caused by strong near field enhancements of sub-micrometer width apertures in THz frequencies have been reported [14]. In order to measure such near field enhancement, electro-optic measurements of THz near field are widely used [12,15,16]. However, direct measurements of the THz near field are technically difficult for extreme sub-wavelength holes, below sub-micrometer size, because the resolution of the near field imaging is usually limited by spot size of the optical probe beam, typically in scale of a few micrometers [12]. Furthermore, samples must be fabricated on a specially oriented detection crystal which can manifest optical properties of metallic holes and the near field distribution [17,18]. On account of those difficulties of direct near field measurement, a new experimental scheme, measurement of the near field enhancement via the far field transmission is proposed [14,19]. Here, the transmission through a finite aperture is used as reference signal, and the near field

enhancement given by a sample can be read from the transmission ratio between signals with and without the sample. By using this method, Seo et al. [14] and Park et al. [19] experimentally determined near field enhancements of 800 at 0.1 THz with a 70-nm-width slit and 200 at 1 THz with a 120- μm -length and 1.8- μm -width rectangular hole, respectively. Since an arbitrary reference aperture can be used for such experiment, a question might arise whether the field enhancement measured in the far field highly depends on a particular choice of the aperture. In this paper, we experimentally demonstrate that near field enhancements of sub-wavelength slits are essentially independent of the reference aperture and are uniquely determined by slits themselves. Additionally, we measure the near field enhancements of single slits with various widths and show that the field enhancement is commonly expressed by inverse frequency dependence and the maximum value of the enhancement for the smallest width slit of 500 nm reaches over 200 at 0.1 THz. This paper is organized as follows: in Section 2 we derive simple relation between the near and the far field enhancements using the Kirchhoff integral formalism and the near field enhancement factor is defined. Our THz experimental set up and processes of the sample preparation are explained in Section 3. In Section 4 the measured near field enhancements of a slit with two apertures are present and reference aperture effects are discussed. Experimental results of the near field enhancement with various slits are shown. Finally, conclusion and summary are offered in Section 5.

2. Kirchhoff integral formalism and the relation between near and far fields

The connection between the near and the far field enhancement is derived from the Kirchhoff integral formalism [20]. Fig. 1 (a) shows

^{*} Corresponding author. Department of Physics and Astronomy, Seoul National University, Gwanakro Sillim-dong, Gwanak-gu, Seoul, 151-747, Republic of Korea. Tel.: +82 2 889 1295; fax: +82 2 884 3002.

E-mail address: kyoung21@snu.ac.kr (J.S. Kyoung).

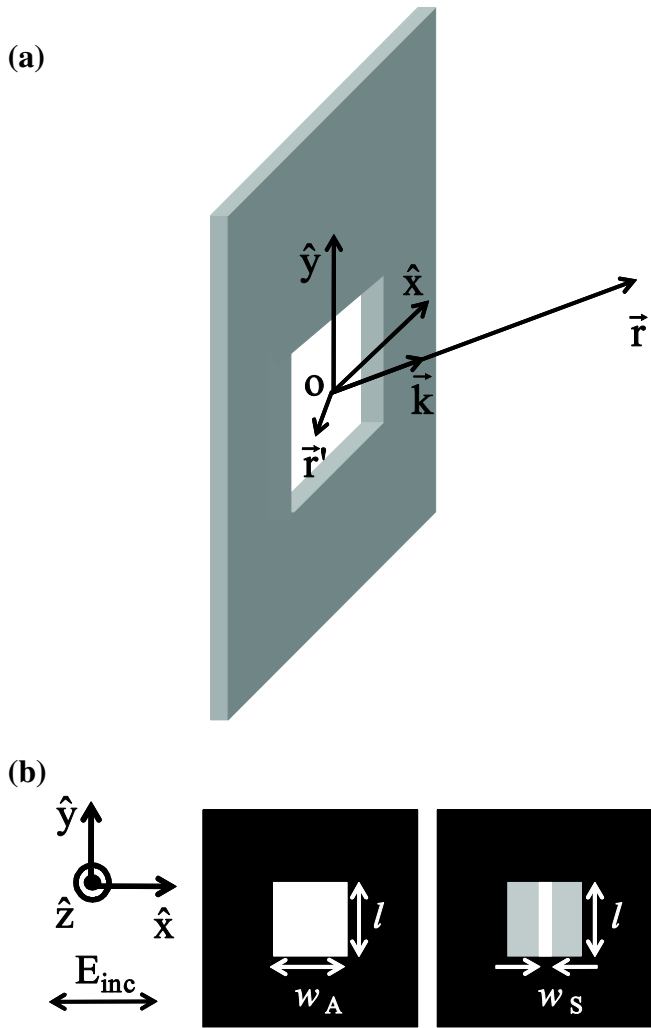


Fig. 1. (a) Diffraction geometry for a plane screen with an aperture at the center. (b) Drawing for a reference aperture only (left) and aperture with a slit sample (right). The incident beam has horizontal direction of polarization.

geometry of our basic diffraction system, a plane metal screen with a rectangular aperture positioned at origin of Cartesian coordinate system. At an observation point located far from the aperture the electric field can be approximated by the Kirchhoff integral [21]:

$$\vec{E}(\vec{r}) = \frac{ie^{ikr}}{2\pi r} \vec{k} \times \int_A \hat{n} \times \vec{E}(\vec{r}') e^{-i\vec{k} \cdot \vec{r}'} da', \tag{1}$$

where A represents the aperture opening, r is the distance from origin O to the observation point, \hat{n} is the surface normal, and \vec{k} is the wave vector in the direction of observation point.

For a THz beam polarized in the horizontal direction (x -axis) and impinging upon the aperture at the normal incidence, we define the transmitted horizontal (x -axis) electric fields only through the reference aperture as E_f^A and through a slit sample attached on the reference aperture as E_f^S , respectively (Fig. 1 (b)). Then, the normalized amplitude $\alpha(\omega)$ is defined by the ratio between two amplitudes:

$\alpha(\omega) \equiv \left| \frac{E_f^S(\omega)}{E_f^A(\omega)} \right|$. According to the Kirchhoff integral formalism, the transmitted amplitude through the aperture, measured at the dif-

fraction center $\mathbf{r} = (0, 0, r)$, is proportional to the x -component of the near field distribution in the aperture E_n^A (Fig. 1 (b)):

$$E_f^A = \frac{e^{ikr}}{i\lambda r} \int_0^{w_A} \int_0^l E_n^A(x', y') dx' dy' = \frac{e^{ikr}}{i\lambda r} \langle E_n^A \rangle w_A l, \tag{2}$$

where the bracket $\langle \rangle$ means the averaged near field over the width w , i.e. $\langle E_n \rangle = \frac{1}{w} \int_0^w E_n(x') dx'$. Unlike the case of the x -component, the averaged y - and z -components of the near field are negligible due to the odd symmetric field distributions in the opening [22], thus can be neglected. In the similar manner, we can express the transmitted far field through the slit E_f^S as

$$E_f^S = \frac{e^{ikr}}{i\lambda r} \int_0^{w_S} \int_0^l E_n^S(x', y') dx' dy' = \frac{e^{ikr}}{i\lambda r} \langle E_n^S \rangle w_S l. \tag{3}$$

By dividing the two equations we obtain a simple relation between the near and the far fields as

$$\frac{\langle E_n^S(\omega) \rangle}{\langle E_n^A(\omega) \rangle} = \frac{\alpha(\omega)}{\beta}, \tag{4}$$

where $\beta = \frac{w_S}{w_A}$ denotes the ratio of widths between the reference aperture and the slit. By considering the field enhancement by the reference aperture with respect to the incident THz beam, $\langle E_n^A(\omega) \rangle = \gamma(\omega) \cdot |E_{inc}(\omega)|$, the near field enhancement factor measured in the far field is finally given as

$$\frac{\langle E_n^S(\omega) \rangle}{\langle E_{inc}(\omega) \rangle} = \frac{\gamma(\omega) \cdot \alpha(\omega)}{\beta}. \tag{5}$$

3. Experimental set up and sample preparation

THz time domain spectroscopy (THz-TDS) is used to measure the near field enhancement for various slit samples. Fig. 2 (a) shows

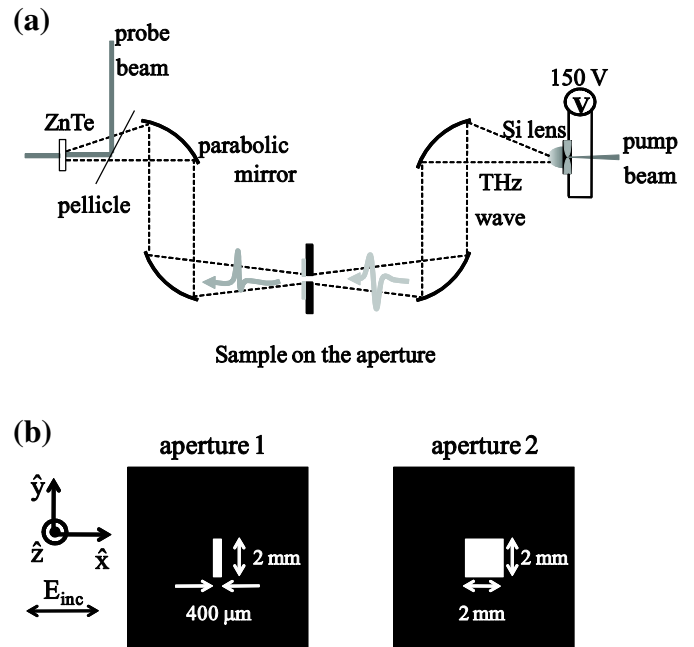


Fig. 2. (a) Terahertz time domain spectroscopy (THz-TDS) set up based on the electro-optic detection. Samples are located at the focal point of the THz beam and transmitted wave through the sample is guided by two parabolic mirrors. (b) Two types of apertures are shown.

schematically our THz-TDS system which has a spectral range from 0.1 THz to 1.1 THz. When a semi-insulating GaAs emitter biased with 50 kHz and 150 V square voltage pulses is illuminated by Ti:sapphire mode-locked laser with the power of 600 mW and pulse width of 150 fs, a single-cycle THz pulse is generated. After passing through a silicon lens, the THz pulse is collected and guided by two parabolic mirrors whose focal lengths are 150 mm and 100 mm, respectively. Samples are located at the THz focus center, and the transmitted THz wave through a sample is guided to the detection part. Electro-optic detection method is used to measure the THz time domain signals [23]. After Fourier transforming time traces, we can acquire transmitted amplitudes and phases in frequency domain.

In our experiments, we use two different widths ($w_A = 400 \mu\text{m}$ and 2 mm) of the reference aperture with a fixed length ($l = 2 \text{ mm}$), to investigate the aperture size effect (Fig. 2 (b)). The metal plates for apertures are thick and wide enough to block the direct THz transmission. We prepare slit samples with diverse widths ($w_S = 450 \mu\text{m}$, $125 \mu\text{m}$, $50 \mu\text{m}$, $23 \mu\text{m}$ and 500 nm). Our micrometer-size single slit samples are made in a $17\text{-}\mu\text{m}$ -thick Al film using laser machining. For the 500 nm slit sample, we first prepare a nearly free standing 60-nm -thick gold film which is deposited onto a $1.2\text{-}\mu\text{m}$ -thick layer of SiO_2 followed by a $0.5\text{-}\mu\text{m}$ -thick SiN. Then, a nano slit is fabricated on the gold film using Focused Ion Beam (FIB) apparatus.

4. Results and discussion

At first, experiments using two different reference apertures (Fig. 2 (b)) with the $50\text{-}\mu\text{m}$ -width slit are performed to check the reference

aperture size effect. Fig. 3 (a) shows the transmitted amplitudes through the slit attached on aperture 1 ($w_A = 400 \mu\text{m}$) and aperture 2 ($w_A = 2 \text{ mm}$), each of which is normalized by the transmitted amplitude through bare apertures 1 and 2, respectively. As clearly seen, transmission amplitudes $\alpha(\omega)$ are quite different to each other. In the overall frequency range, the normalization with the aperture 1 gives a larger transmission, because the reference signal of the smaller aperture $E_1^A(\omega)$ is lesser than that of the bigger one. Fig. 3 (b) represents the incident electric field enhancements $\gamma(\omega)$ by reference apertures 1 and 2, calculated with single mode diffraction theory [17]. We verify, using the finite difference time domain (FDTD) method, that our model gives less than 5% errors in the desired frequency range. For the aperture 1 the incident electric field is largely enhanced at low frequencies while no enhancement is observed at higher frequencies. We numerically observe that the aperture 2 gives almost no enhancements, $\gamma(\omega) \approx 1$, in the considered spectral region.

Now, we estimate the near field enhancement of the $50\text{-}\mu\text{m}$ -width slit sample using measured $\alpha(\omega)$ and calculated $\gamma(\omega)$ with gap-to-aperture width ratio $\beta = 0.125$ and 0.025 for the apertures 1 and 2, respectively, through Eq. (5). Fig. 4 (a) shows the enhancement factors of the slit for two different reference apertures. All in all, the enhancement factors are almost independent of particular choice of the reference apertures that we used. As a result, we can determine the near field enhancement factor only given by the slit itself, excluding the influence by the reference aperture.

With these calibrated reference apertures, next, we measure the near field enhancements of slits with different widths ranging from $450 \mu\text{m}$ all the way down to 500 nm . We use a $2 \text{ mm} \times 2 \text{ mm}$ size

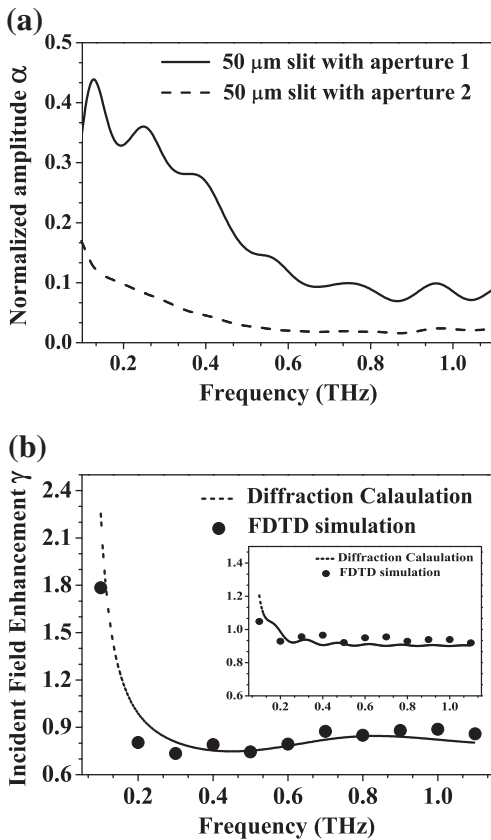


Fig. 3. (a) The normalized-against-the aperture amplitude $\alpha(\omega)$ using apertures 1 and 2, respectively. Normalized amplitude with aperture 1 gives a larger transmission than that with aperture 2 in overall frequency regime. (b) The incident electric field enhancement $\gamma(\omega)$ by reference aperture 1 ($l = 2 \text{ mm}$ and $w_A = 400 \mu\text{m}$) is calculated with both diffraction theory and FDTD simulation. Inset: the incident field enhancement due to aperture 2 ($l = 2 \text{ mm}$ and $w_A = 2 \text{ mm}$).

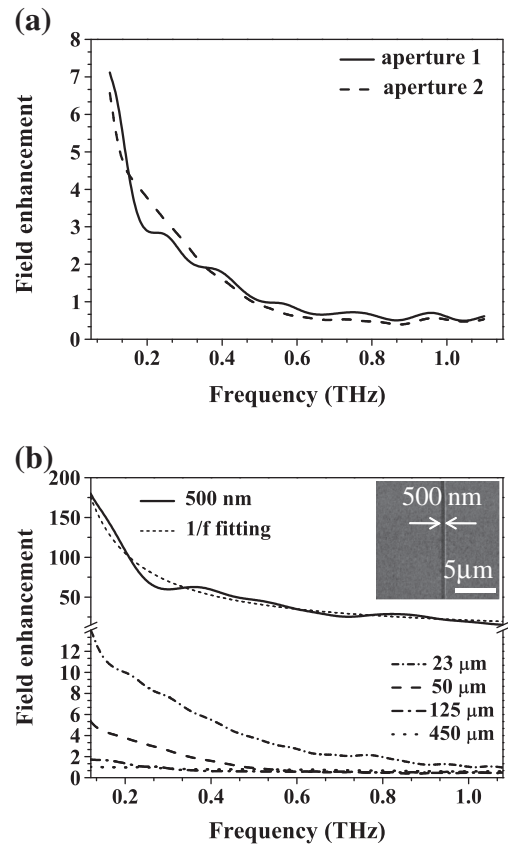


Fig. 4. (a) Near field enhancement for a $50\text{-}\mu\text{m}$ -width slit using aperture 1 (dash) and aperture 2 (solid), showing that the enhancement is largely independent of the normalizing apertures. (b) Field enhancement of various slits keeps increasing with decreasing slit widths and follows inverse frequency dependence with the 500-nm -width slit. Inset: 500 nm slit SEM image.

aperture as a reference. The field enhancements through slits increase as the width of the slit decreases (Fig. 4 (b)). The inverse frequency dependence of the field enhancement by narrow slits has been studied in several papers [14,24,25]. In our experiment, the maximum field enhancement reaches 200 at 0.1 THz with the 500-nm-width slit.

5. Conclusion

In this study we experimentally demonstrate that the near field enhancement of sub-wavelength slits can be measured in the far field by using a reference aperture. Through explicitly considering the aperture effect, the near field enhancement of slits is completely free from the choice of the aperture and only decided by slits themselves. Using this method, we observe two orders of amplitude enhancement by a $\lambda/6000$ sub-wavelength slit fabricated on a metal film, compared to the incident electric field. Hugely enhanced THz electric field by extreme sub-wavelength holes can be used for various researches such as THz-nonlinear measurements, single molecule detection, and THz active switching devices.

Acknowledgements

This research was supported by the Korea Science and Engineering Foundation (KOSEF) (SRC, No: R11-2008-095-01000-0) and the Korea Research Foundation (KRF) grant funded by the Korea government (MEST) (No: 2009-0071309), KICOS (GRL, K2081500003), Seoul Science Fellowship and the Seoul R&BD Program (10543).

References

- [1] C. Genet, T.W. Ebbesen, *Nature* 445 (2007) 39.
- [2] E. Popov, M. Nevière, S. Enoch, R. Reinisch, *Phys. Rev. B* 62 (2000) 16100.
- [3] W.L. Barnes, W.A. Murray, J. Dintinger, E. Devaux, T.W. Ebbesen, *Phys. Rev. Lett.* 92 (2004) 107401.
- [4] F.J. García de Abajo, R. Gómez-Medina, J.J. Sáenz, *Phys. Rev. E* 72 (2005) 016608.
- [5] J. Lee, M. Seo, D. Park, D. Kim, S. Jeoung, C. Lienau, Q.H. Park, P. Planken, *Opt. Express* 14 (2006) 1253.
- [6] D.J. Park, S.B. Choi, Y.H. Ahn, Q.H. Park, D.S. Kim, *J. Korean Phys. Soc.* 54 (2009) 64.
- [7] J.W. Lee, M.A. Seo, J.Y. Sohn, D.J. Park, Y.H. Ahn, D.S. Kim, *J. Korean Phys. Soc.* 48 (2006) 103.
- [8] J.W. Lee, M.A. Seo, D.H. Kang, K.S. Khim, S.C. Jeoung, D.S. Kim, *Phys. Rev. Lett.* 99 (2007) 137401.
- [9] K.J.K. Koerkamp, S. Enoch, F.B. Segerink, N.F. van Hulst, L. Kuipers, *Phys. Rev. Lett.* 92 (2004) 183901.
- [10] K.L. van der Molen, K.J. Klein Koerkamp, S. Enoch, F.B. Segerink, N.F. van Hulst, L. Kuipers, *Phys. Rev. B* 72 (2005) 045421.
- [11] H. Cao, A. Nahata, *Opt. Express* 12 (2004) 3664.
- [12] M.A. Seo, A.J.L. Adam, J.H. Kang, J.W. Lee, K.J. Ahn, Q.H. Park, P.C.M. Planken, D.S. Kim, *Opt. Express* 16 (2008) 20484.
- [13] F.J. García-Vidal, E. Moreno, J.A. Porto, L. Martín-Moreno, *Phys. Rev. Lett.* 95 (2005) 103901.
- [14] M.A. Seo, H.R. Park, S.M. Koo, D.J. Park, J.H. Kang, O.K. Suwal, S.S. Choi, P.C.M. Planken, G.S. Park, N.K. Park, Q.H. Park, D.S. Kim, *Nat. Photonics* 3 (2009) 152.
- [15] A.J.L. Adam, J.M. Brok, P.C.M. Planken, M.A. Seo, D.S. Kim, *C.R. Phys.* 9 (2008) 161.
- [16] A.J.L. Adam, J.M. Brok, M.A. Seo, K.J. Ahn, D.S. Kim, J.H. Kang, Q.H. Park, M. Nagel, P.C.M. Planken, *Opt. Express* 16 (2008) 7407.
- [17] J.H. Kang, J.-H. Choe, D.S. Kim, Q.H. Park, *Opt. Express* 17 (2009) 15652.
- [18] L. Guestin, A.J.L. Adam, J.R. Knab, M. Nagel, P.C.M. Planken, *Opt. Express* 17 (2009) 17412.
- [19] D.J. Park, S.B. Choi, Y.H. Ahn, F. Rotermund, I.B. Sohn, C. Kang, M.S. Jeong, D.S. Kim, *Opt. Express* 17 (2009) 12493.
- [20] M. Born, E. Wolf, *Principles of Optics*, 7 ed. Cambridge University Press, Cambridge UK, 1999.
- [21] J.D. Jackson, *Classical Electro Dynamics*, 3 ed. John Wiley & Sons, 2007.
- [22] C. Butler, Y. Rahmat-Samii, R. Mittra, *IEEE Trans. Antennas Propag.* 26 (1978) 82.
- [23] G. Gallot, D. Grischkowsky, *J. Opt. Soc. Am. B* 16 (1999) 1204.
- [24] J.H. Kang, D.S. Kim, Q.-H. Park, *Phys. Rev. Lett.* 102 (2009) 093906.
- [25] R. Harrington, D. Auckland, *IEEE Trans. Antennas Propag.* 28 (1980) 616.